Journal of Biomechanics 178 (2025) 112423

Contents lists available at ScienceDirect

Journal of Biomechanics

journal homepage: www.elsevier.com/locate/jbiomech

Perspective article

Modeling implications of the relationship between active and passive skeletal muscle mechanical properties

Richard L. Lieber [a,b,c,*], Zheng Wang [d], Benjamin I. Binder-Markey [a,e], Lomas S. Persad [d], Alexander Y. Shin [d], Kenton R. Kaufman [d]

[a] Shirley Ryan AbilityLab, Chicago, IL, United States
[b] Hines V.A. Hospital, Maywood, IL, United States
[c] Northwestern University, Chicago, IL, United States
[d] Mayo Clinic, Rochester, MN, United States
[e] Drexel University, Philadelphia, PA, United States

ARTICLE INFO

Keywords:
Muscle architecture
Muscle modeling
Orthopaedic surgery
Tendon slack length

ABSTRACT

It is challenging to obtain *in vivo* or *in situ* experimental data from human muscles due to the invasive nature of such measurements. As a result, many investigations of human performance, surgery, or skeletal adaptation are necessarily based on musculoskeletal models. The utility of such models will depend on the question being asked and the extent to which the model is sufficiently accurate to address that question. In this perspective article, we take advantage of unique intraoperative access to the human gracilis muscle and make direct comparisons between commonly modeled parameters and those measured from the human gracilis. We directly compare muscle–tendon unit (MTU) length, optimal fiber length, and tendon slack length. Our results demonstrate that measured and modeled length parameters differ greatly. This is primarily due to the fact that slack muscle length and optimal muscle length differ greatly for the human gracilis and that models assume they are the same length.

1. Introduction

Understanding human muscle performance is of great importance in many fields such as sports medicine, orthopaedic surgery, exercise science, neurology and rehabilitation. Such an understanding is provided, in part, using preclinical models, primarily rodents, which are then extrapolated to the human condition. This is because obtaining actual experimental muscle data from humans is extremely challenging due to its invasive nature. Thus, many investigators rely on musculoskeletal modeling to fill the gap between directly measured properties and theoretical constructs. Progress in this field has been made recently in terms of graphical representation of movement and computation efficiency, but it is important to continue to press for validation studies that will produce accurate predictions that enable progress in the field of biomechanics (Hicks et al., 2015).

2. Overview of human muscle modeling

The typical approach used to model human performance is to define the relevant structural features (usually muscles, tendons, ligaments and bones), ascribe appropriate material and physiological properties to these structures and develop equations of motion that interconnect them all (Seth et al., 2018). A major advance in this approach was enabled by a seminal contribution to the literature from Felix Zajac (Zajac, 1989). Zajac created a generic muscle–tendon unit model whereby a muscle fiber is placed in series with a tendon at some pennation angle (Fig. 1). This model allowed a single system of equations to represent the complexity and variety of muscle–tendon functions by scaling the model to any particular muscle's structural features. When examining upper extremity (Lieber et al., 1990; Lieber et al., 1992; Murray et al., 2000; Saul, 2015) and lower extremity (Ward et al., 2009; Wickiewicz et al., 1983) muscles, it was clear that various muscles had different fiber length:muscle length ratios that represent each muscle's "relative design" for excursion or velocity. Similarly, muscle–tendon units across the body had different fiber length:tendon length ratios that could suit a muscle more for energy storage, fiber shortening or even absorbing eccentric contractions, thereby potentially preventing injury (Biewener, 2005; Pollock and Shadwick, 1994; Roberts and Marsh, 2003; Shadwick, 1990; Ward et al., 2006). Finally, Zajac coined a term that he called "tendon slack length," which was an offset that allowed a muscle to

* Corresponding author at: Shirley Ryan AbilityLab, 355. E. Erie St, Chicago, IL 60611, USA.
E-mail address: rlieber@sralab.org (R.L. Lieber).

https://doi.org/10.1016/j.jbiomech.2024.112423
Accepted 7 November 2024
Available online 9 November 2024
0021-9290/Published by Elsevier Ltd.

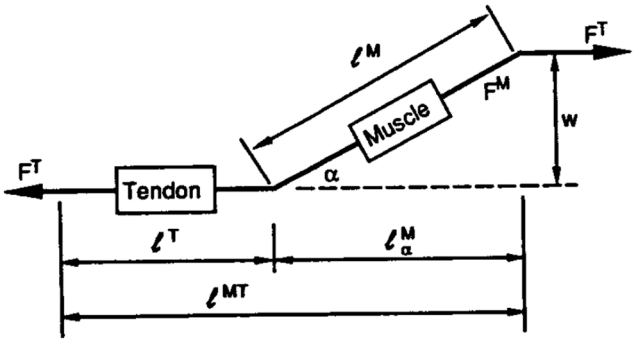

Fig. 1. Schematic representation of a muscle–tendon unit (MTU). In this scheme muscle fibers are arranged at a pennation angle, α, relative to the axis of force generation (from Fig. 20 of Zajac, 1989). Terms in this figure are: L^{MT}, length of the MTU; L^M, length of the muscle fibers; α, pennation angle; L^T, slack tendon length; L^M_α, length of the muscle based on fibers at pennation angle, α; w, muscle width; F^T, tendon force; F^M, muscle force.

operate on the appropriate portion of its length-tension curve that would match experimental joint torque predictions. In practice, tendon slack length is calculated using optimization, where predictions are systematically varied to fit experimental data and it thus becomes a sort of "fudge factor."(Hicks et al., 2015; Murray et al., 2000; Saul et al., 2015). Because of the elegance and simplicity of this model, it has become the conceptual underpinning of many musculoskeletal models.

3. Active and passive muscle Mechanics

Underlying Zajac's muscle–tendon unit model are the muscle's contractile properties (Fig. 2). The active isometric contractile properties reflect intrinsic sarcomere length-tension properties (Edman, 1966; Gordon et al., 1966), scaled to a whole muscle (Winters et al., 2011). The passive length-tension curve (Fig. 2A) represents the passive load bearing structures in the muscle such as connective tissue elements (Huijing and Ettema, 1988; Morgan, 1976; Purslow, 1989), intracellular load-bearing proteins such as titin (Granzier and Irving, 1995; Labeit and Kolmerer, 1995), and the intermediate filament system (Lazarides, 1980). Dynamically, isotonic contractile properties are described by the force–velocity curve (Fig. 2B) whereby muscle force decreases hyperbolically with shortening velocity (Hill, 1953) and abruptly increases upon forced lengthening (Katz, 1939).

While the basic forms of active isometric and isotonic relationships described above have been validated across a variety of species and at a variety of scales, quantifying the passive mechanical properties of muscle is more problematic (Winters et al., 2011). This is because, unlike the active length-tension curve, which represents a scaled version of the sarcomere length-tension curve, there is no equivalent structural underpinning that provides a high resolution passive muscle structure–function correlation. For example, in a recent multiscale study of three different rabbit muscles, we clearly showed that, while the isolated muscle fiber passive length-tension relationship was very consistent across muscles, as scale increased to bundles, fascicles and whole muscles, each of the three muscles studied yielded a quite different scaling relationship (Ward et al., 2020), presumably based on their different connective tissue structures (Binder-Markey et al., 2020). This variability was especially pronounced at the fascicular level (see open squares in Fig. 2A, 2B and 2C of Ward et al., 2020). Differences amongst muscles were not explained by differences in the titin isoform and only marginally by differences in collagen content (see Fig. 5 of Ward et al., 2020). In a separate comparison of these same three rabbit muscles, while the active length-tension relationship for all muscles scaled well based on the rabbit sarcomere length-tension curve and each muscle's architectural properties, the passive curve did not fit nearly as well nor as consistently (see dashed lines in Fig. 2 of Winters et al., 2011).

In the context of this perspective paper, it is becoming clear that one of the most important assumptions made in the generic model of Zajac (Fig. 2) was that the length at which muscle force was optimal was assumed to be the same length at which the muscle was slack (arrows, Fig. 2A). While this constraint allows creation of models where the joint moment is explained by muscle active and passive properties, it is not clear whether the underlying active and passive muscle properties that produce the moment are accurate. Does this assumed relationship between active and passive properties hold for human muscles? What are the implications for muscle modeling and our understanding of human movement if it does not?

4. Direct measurement of human muscle properties

To address these questions, for the past several years, we have exploited our nearly unprecedented access to the human gracilis muscle to make direct measurements of its passive (Persad et al., 2021b) and active (Binder-Markey et al., 2023) properties. This is accomplished by working with our surgical colleagues during a unique muscle transplantation surgery in which the gracilis muscle is transplanted from the

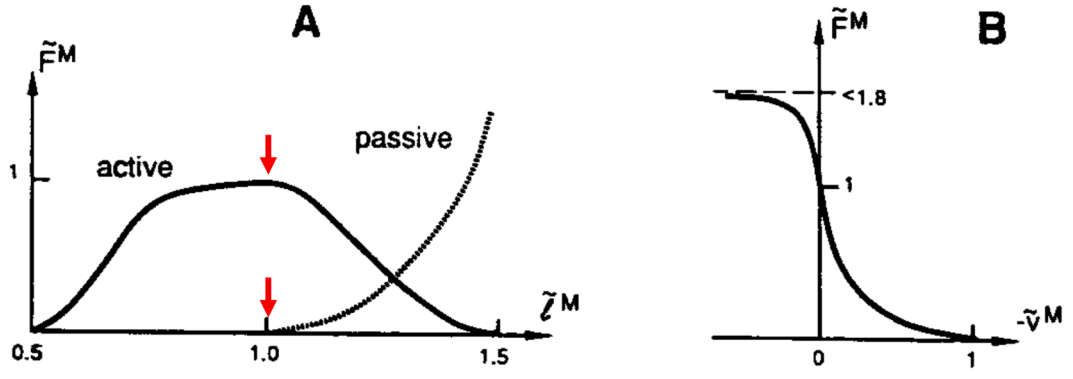

Fig. 2. Generic representation of muscle physiological properties. (A) Isometric length-tension properties of muscle in the active (solid line) and passive (dotted line) conditions. These data are on a normalized scale whereby normalized muscle force ($\tilde{F}^M$) ranges from 0 (passive) to 1 (maximum) and optimal muscle force (red arrow) and slack length occur at the same normalized length ($\tilde{L}^M$; red arrow; modified from Fig. 8 of Zajac, 1989). (B) Isotonic force–velocity relationship whereby normalized muscle force ($\tilde{F}^M$) ranges from 0 (at normalized maximum velocity, ($\tilde{V}^M$) to 1 (at zero velocity) to 1.8 under conditions of active lengthening eccentric contractions (negative velocity). (For interpretation of the references to colour in this figure legend, the reader is referred to the web version of this article.)

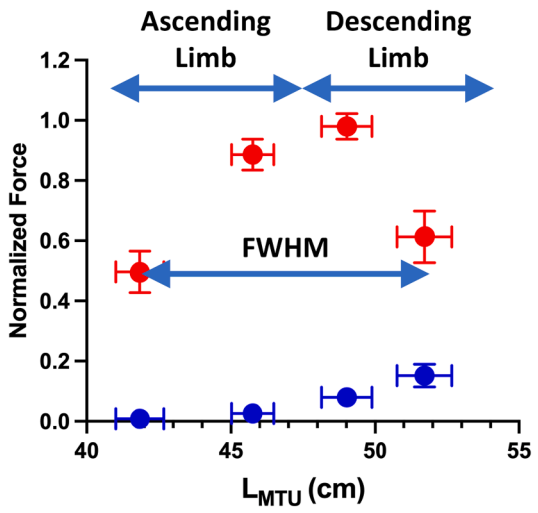

Fig. 3. Human gracilis active (red symbols) and passive (blue symbols) length-tension properties. This figure graphically illustrates the width of the length-tension curve expressed as full-width at half maximum (FWHM) that allows fiber length calculation using the equation:$L_{fopt}(mm) = 0.68{*}FWHM(mm)$ (Figure modified from Binder-Markey et al., 2023). (For interpretation of the references to colour in this figure legend, the reader is referred to the web version of this article.)

Table 1
Abbreviations Used.

List of Abbreviations.	
FWHM	Full width of length-tension curve at half of maximum force
F^T	Force measured at tendon (Fig. 1)
F^m	Force generated by the muscle (Fig. 1)
L^M	Muscle length (Fig. 1)
L^M_α	Muscle length based on the fiber pennation angle (Fig. 1)
L^F	Length of the muscle fibers
L^F_{opt}	Length of muscle fibers at optimal force generation
L^{MT}	Length of the muscle–tendon unit (MT)
L^{MT}_{opt}	Length of the muscle–tendon unit at optimal muscle fiber length
L^{MT}_{slack}	Length of the muscle–tendon unit while slack
L^T_{slack}	Length of the tendon while slack
L^T	External tendon length (Fig. 1)
W	Width of muscle (Fig. 1)

medial thigh along with its nerve and blood supplies into the biceps brachii bed of the arm to restore elbow flexion. After 1–2 years of reinnervation, the gracilis replaces the function of the biceps (Giuffre et al., 2012). After exposure and just prior to gracilis transplantation, a small buckle transducer (An et al., 1990) is placed on the distal gracilis insertion tendon at the proximal medial tibia to measure muscle force (see Fig. 10 inset of Persad et al., 2022). Then, the gracilis is placed in a shortened *in vivo* position and lengthened stepwise in three successive positions with increasing knee extension and hip abduction (see Fig. 1 of Persad et al., 2023). The resulting active (red symbols, Fig. 3) and passive muscle tension (blue symbols, Fig. 3) encompass the majority of the gracilis' functional length-tension curve. A clear ascending and descending limb are seen (Gordon et al., 1966) and high resolution active and passive forces are measured with a signal-to-noise ratio of at least 50 (Persad et al., 2022). The four active data points from each patient are fit to a second order polynomial (Binder-Markey et al., 2023) and the full width at half maximum (FWHM) is used to calculate the optimal fiber length (L^F_{opt}) for that patient—the length at which active muscle force is maximum. This length is calculated using the equation (see abbreviations in Table 1):

$$L^F_{opt}(cm) = 0.68{*}FWHM(cm) \quad (1)$$

which was derived previously from experimental measurement of 11 different muscles across four different species (see Fig. 4 of Winters et al., 2011). During transfer, the entire gracilis MTU, including its full proximal tendon and distal tendon, is placed on a sterile towel being gently laid from origin to insertion, yielding the actual, physical, muscle–tendon unit slack length (L^{MT}_{slack})(Fig. 4). *Note that, in this case, MTU slack length is not a fudge factor at all, but a real, measured anatomical parameter.*

Given that we had high resolution values for many anatomical parameters, we also modeled these anatomical lengths using standard modeling software, OpenSim v4.4 (Seth et al., 2018; Zajac, 1989), based on Zajac's muscle model. The default muscle model parameters of optimal fiber length and tendon slack length (Hamner et al., 2010) were scaled to that patient's height as detailed previously (Persad et al., 2021a).

5. Comparison between experimental and modeled muscle parameters

Experimentally measured L^{MT}_{slack} was significantly shorter compared to the model prediction, only 81 % of the modeled value (Fig. 5A, white bar

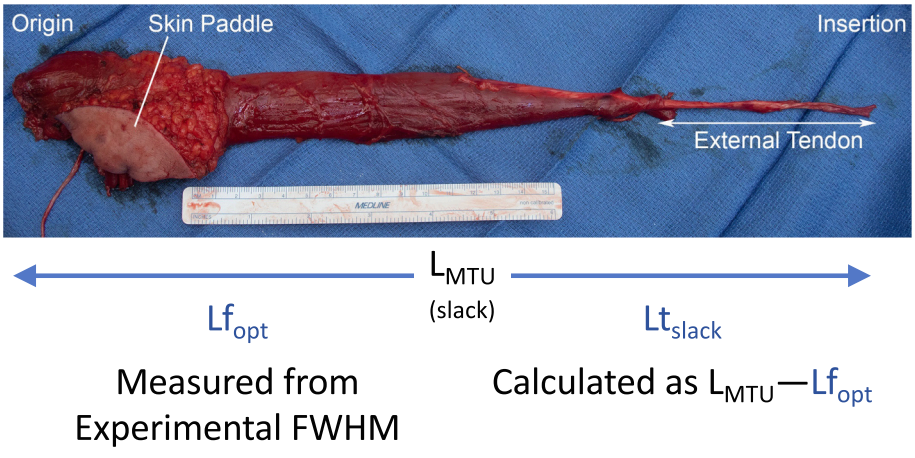

Fig. 4. Intraoperative view of human gracilis muscle on sterile towel after excision from medial thigh and prior to transplantation into the biceps bed. This condition represents the actual slack length of this muscle–tendon unit (modified from Persad et al., 2022). Tendon slack length is calculated from this value.

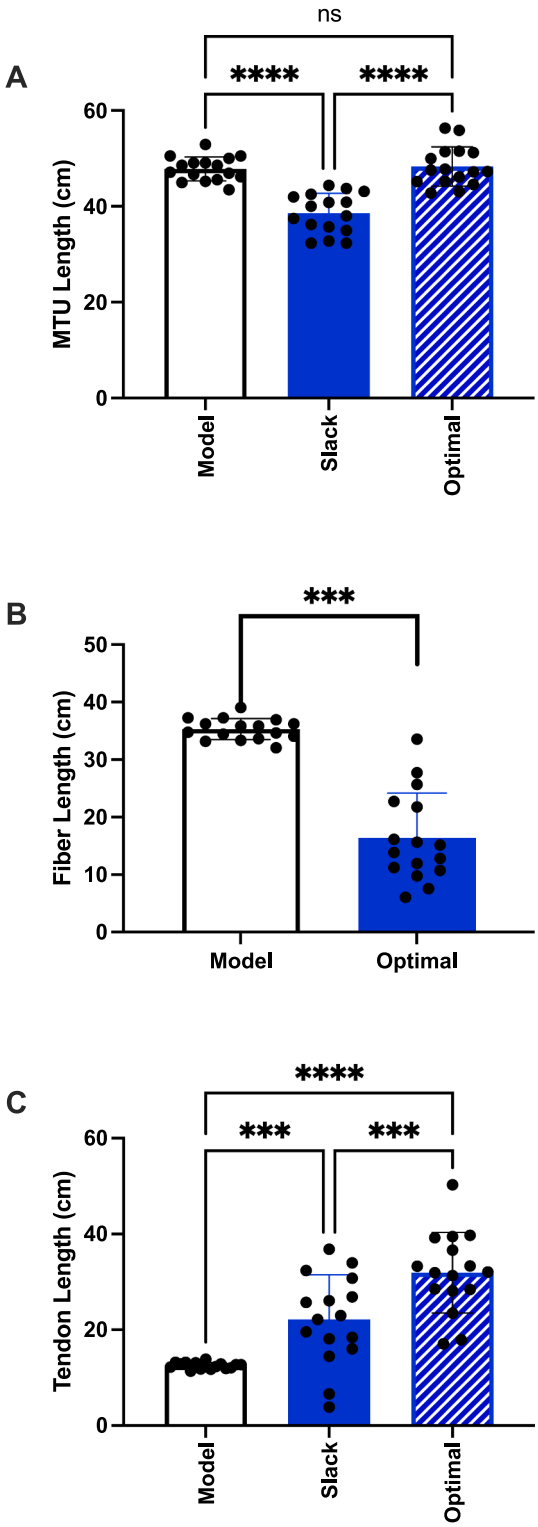

Fig. 5. Comparison between experimental and modeled data. (A) Muscle-tendon unit length, (B) Optimal fiber length, (C) Tendon length. Experimentally, measured values (blue bars) are compared to modeled values (white bars). Hatched bars in (A) and (C) represent alternate approaches to calculating these parameters as described in the text. Note that, except for MTU length at optimal length, there are significant differences between experimental and modeled data. (Statistical significance levels: **, $p < 0.01$; ***, $p < 0.001$; ****, $p < 0.0001$). (For interpretation of the references to colour in this figure legend, the reader is referred to the web version of this article.)

vs. blue bar). Since, as described above, most skeletal muscle models assume that the L^{MT}_{slack} is equal to muscle–tendon unit length where L^{F} is optimal (L^{MT}_{opt}), we also calculated experimental L^{MT}_{opt} as the peak of the second order polynomial. Our experimental L^{MT}_{opt} was not significantly different from the modeled value (Fig. 5A, white bar vs. hatched bar). Calculated L^{F}_{opt} was significantly lower ($p < 0.001$), only 46 % of that predicted by the model (Fig. 5B). (Since this experimental length only occurs at optimal fiber length, it is not possible to calculate a "slack" optimal fiber length.) The underlying basis for the large discrepancy between measured and predicted L^{F}_{opt} is not currently known. However, we suspect that the actual anatomical muscle cells (fibers) in long human muscles such as the gracilis are much shorter than the fascicle lengths we previously measured using dissections from whole muscle (Son et al., 2024; Ward et al., 2009). Current studies, beyond the scope of this perspective paper, are underway to investigate this issue.

Our experimental L^{MT}_{slack} was clearly not equal to L^{MT}_{opt} as assumed by most models. What about the associated values for tendon slack length? We took two approaches to calculate tendon slack length (L^{T}_{slack}) (Equations (2) and (3) below) since it would be reasonable to use either approach in a modeling exercise. The two approaches are:

$$L^{T}{}_{1}(cm) = L^{MT}_{slack}(cm) - L^{F}_{opt}(cm) \tag{2}$$

$$L^{T}{}_{2}(cm) = L^{MT}_{opt}(cm) - L^{F}_{opt}(cm) \tag{3}$$

Each approach uses a different MTU "reference" length from which to subtract L^{F}_{opt}.

Unfortunately, in either case, L^{T}_{slack} greatly exceeded that predicted by the model by more than 100 % ($p < 0.001$; Fig. 5C). Thus, while it is possible to use different assumptions to adjust modeled MTU length to fit experimental data, no set of assumptions yields a value for either L^{F}_{opt} or L^{T}_{slack} that resemble the actual experimental values.

6. Summary

This disparity between intraoperative measurements and model predictions of human gracilis muscle properties clearly demonstrates that modeled parameters may not reflect anatomical reality. One of the most obvious reasons for this disparity is that, for most skeletal muscles, optimal muscle length is longer than slack muscle length. This has been demonstrated in cats (Tabary et al., 1976), rabbits (Winters et al., 2011), mice (Warren et al., 1999), rats (Pierotti et al., 1990), guinea pig (Powell et al., 1984), fish (Rome et al., 1993) and now, humans (Binder-Markey et al., 2023). Intraoperative experience is that, with joints in a neutral position, all muscle–tendon units retract when released from their insertion point. This clearly demonstrates that the true slack length of the human MTU is shorter than its *in vivo* length.

Discarding the modeling assumption that $L^{MT}_{slack} = L^{MT}_{opt}$ is problematic because it adds an additional degree of freedom to any model and its value is completely unknown. This results in an optimization process that has too many parameters to vary which results in overfitting in most cases. As mentioned above, uncertainty regarding L^{MT}_{slack} results from the fact that the passive sarcomere length-tension and passive muscle length-tension relationships do not have a clear structural basis in contrast to the active sarcomere length-tension relationship elucidated over 50 years ago (Gordon et al., 1966). This incomplete understanding of the structural basis for passive force in muscle and a systematic review of passive muscle mechanical properties have recently been presented (Binder-Markey et al., 2021; Lieber and Meyer, 2023). In short, the reason for the uncertainty in knowing passive muscle force results from our incomplete understanding of the structural basis of passive force generation in skeletal muscle. Future studies must be directed toward a more complete understanding of this phenomenon to allow the

biomechanics community to model human muscle function accurately.

7. Limitations

This perspective paper provides only a single explicit comparison for a single muscle at a single center. As such, it is not clear the extent to which these large errors in musculoskeletal models generalize to other human muscles. In addition, not all comparisons between experiment and theory (Fig. 5) perfectly align with the theoretical models. For example, at optimal muscle length under active force conditions, tendon strains, which can alter muscle force, but this is not included in any of our simulations. For this particular system, in which the tendons are relatively stiff, this would not substantially affect our comparisons as this would only alter tendon lengths by 1–3 %, which is well within the variation of the current samples and model. Finally, we recently presented physiological data of optimal fiber lengths (Binder-Markey et al., 2023) that strongly contrast with our anatomical data previously published (Ward et al., 2009). Our initial sense is that this disparity applies primarily to very long human muscles, but this impression has not yet been experimentally tested. Both of these optimal fiber lengths (physiological and anatomical) were used and considered within this perspective.

CRediT authorship contribution statement

Richard L. Lieber: Writing – original draft, Visualization, Validation, Supervision, Resources, Project administration, Methodology, Investigation, Funding acquisition, Formal analysis, Data curation, Conceptualization. **Zheng Wang:** Writing – review & editing, Writing – original draft, Validation, Methodology, Formal analysis, Data curation. **Benjamin I. Binder-Markey:** Writing – review & editing, Writing – original draft, Validation, Methodology, Investigation, Formal analysis. **Lomas S. Persad:** Writing – review & editing, Writing – original draft, Investigation, Data curation. **Alexander Y. Shin:** . **Kenton R. Kaufman:** Writing – review & editing, Writing – original draft, Validation, Supervision, Project administration, Investigation, Funding acquisition, Conceptualization.

Declaration of competing interest

The authors declare that they have no known competing financial interests or personal relationships that could have appeared to influence the work reported in this paper.

Acknowledgements

This work was supported in part by Research Career Scientist Award Number IK6 RX003351 and Merit Review I01 RX002462-from the United States (U.S.) Department of Veterans Affairs Rehabilitation R&D (Rehab RD) Service. We appreciate the constructive critique from anonymous reviewers.

References

An, K.-N., Berglund, L., Cooney, W.P., Chao, E.Y.S., Kovacevic, N., 1990. Direct in-vivo tendon force measurement system. J. Biomech. 23, 1269–1271.
Biewener, A.A., 2005. Biomechanical consequences of scaling. J Exp Biol 208, 1665–1676.
Binder-Markey, B.I., Broda, N.M., Lieber, R.L., 2020. Intramuscular anatomy drives collagen content variation within and between muscles. Front Physiol 11, 293.
Binder-Markey, B.I., Sychowski, D., Lieber, R.L., 2021. Systematic review of skeletal muscle passive mechanics experimental methodology. J Biomech 129, 110839.
Binder-Markey, B.I., Persad, L.S., Shin, A.Y., Litchy, W.J., Kaufman, K.R., Lieber, R.L., 2023. Direct intraoperative measurement of isometric contractile properties in living human muscle. J Physiol 601, 1817–1830.
Edman, K., 1966. The relation between sarcomere length and active tension in isolated semitendinosus fibres of the frog. J. Physiol. 183, 407–417.
Giuffre, J.L., Bishop, A.T., Shin, A.Y., 2012. Harvest of an entire gracilis muscle and tendon for use in functional muscle transfer: a novel technique. J Reconstr Microsurg 28, 349–358.
Gordon, A.M., Huxley, A.F., Julian, F.J., 1966. The variation in isometric tension with sarcomere length in vertebrate muscle fibres. J. Physiol. (Lond.) 184, 170–192.
Granzier, H., Irving, T., 1995. Passive tension in cardiac muscle: contribution of collagen, titin, microtubules, and intermediate filaments. Biophys. J . 68, 1027–1044.
Hamner, S.R., Seth, A., Delp, S.L., 2010. Muscle contributions to propulsion and support during running. J Biomech 43, 2709–2716.
Hicks, J.L., Uchida, T.K., Seth, A., Rajagopal, A., Delp, S.L., 2015. Is my model good enough? Best practices for verification and validation of musculoskeletal models and simulations of movement. J Biomech Eng 137, 020905.
Hill, A.V., 1953. The mechanics of active muscle. Proc. R. Soc. Lond. B 141, 104–117.
Huijing, P.A., Ettema, G., 1988. Length-force characteristics of aponeurosis in passive muscle and during isometric and slow dynamic contractions of rat gastrocnemius muscle. Acta Morphol. Neerl. Scand. 26, 51–62.
Katz, B., 1939. The relation between force and speed in muscular contraction. J. Physiol. (Lond.) 96, 45–64.
Labeit, S., Kolmerer, B., 1995. Titins: Giant proteins in charge of muscle ultrastructure and elasticity. Science (washington) 270, 293–296.
Lazarides, E., 1980. Intermediate filaments as mechanical integrators of cellular space. Nature (London) 283, 249–256.
Lieber, R.L., Fazeli, B.M., Botte, M.J., 1990. Architecture of selected wrist flexor and extensor muscles. Journal of Hand Surgery. American 15A, 244–250.
Lieber, R.L., Jacobson, M.D., Fazeli, B.M., Abrams, R.A., Botte, M.J., 1992. Architecture of selected muscles of the arm and forearm: anatomy and implications for tendon transfer. Journal of Hand Surgery. American 17A, 787–798.
Lieber, R.L., Meyer, G.A., 2023. Structure-function relationships in skeletal muscle extracellular matrix. J Biomech.
Morgan, D.L., 1976. Separation of active and passive components of short-range stiffness of muscle. Am. J. Physiol. 232, C45–C49.
Murray, W.M., Buchanan, T.S., Delp, S.L., 2000. The isometric functional capacity of muscles that cross the elbow. J Biomech 33, 943–952.
Persad, L.S., Ates, F., Shin, A.Y., Lieber, R.L., Kaufman, K.R., 2021. Measuring and modeling in vivo human gracilis muscle-tendon unit length. J Biomech 125, 110592.
Persad, L.S., Ates, F., Evertz, L.Q., Litchy, W.J., Lieber, R.L., Kaufman, K.R., Shin, A.Y., 2022. Procedures for obtaining muscle physiology parameters during a gracilis free-functioning muscle transfer in adult patients with brachial plexus injury. Sci Rep 12, 6095.
Persad, L.S., Binder-Markey, B.I., Shin, A.Y., Lieber, R.L., Kaufman, K.R., 2023. American Society of Biomechanics Journal of Biomechanics Award 2022: Computer models do not accurately predict human muscle passive muscle force and fiber length: Evaluating subject-specific modeling impact on musculoskeletal model predictions. J Biomech 159, 111798.
Persad, L.S., Binder-Markey, B.I., Shin, A.Y., Kaufman, K.R., Lieber, R.L., 2021b. In vivo human gracilis whole-muscle passive stress-sarcomere strain relationship. J Exp Biol 224.
Pierotti, D.J., Roy, R.R., Flores, V., Edgerton, V.R., 1990. Influence of 7 days of hindlimb suspension and intermittent weight support on rat muscle mechanical properties. Aviat Space Environ Med 61, 205–210.
Pollock, C.M., Shadwick, R.E., 1994. Allometry of muscle, tendon, and elastic energy storage capacity in mammals. Am J Physiol 266, R1022–R1031.
Powell, P.L., Roy, R.R., Kanim, P., Bello, M., Edgerton, V.R., 1984. Predictability of skeletal muscle tension from architectural determinations in guinea pig hindlimbs. J. Appl. Physiol. 57, 1715–1721.
Purslow, P.P., 1989. Strain-induced reorientation of an intramuscular connective tissue network: implications for passive muscle elasticity. J Biomech 22, 21–31.
Roberts, T.J., Marsh, R.L., 2003. Probing the limits to muscle-powered accelerations: lessons from jumping bullfrogs. J Exp Biol 206, 2567–2580.
Rome, L.C., Swank, D., Corda, D., 1993. How fish power swimming. Science (washington d.c.) 261, 340–343.
Saul, K.R., Xiao, Hu., Goehler, C.M., Vidt, M.E., Daly, M., Velisar, A., Murray, W.M., 2015. Benchmarking of dynamic simulation predictions in two software platforms using an upper limb musculoskeletal model. Comput. Methods Biomech. Biomed. Eng. 18, 1445–1458.
Seth, A., Hicks, J.L., Uchida, T.K., Habib, A., Dembia, C.L., Dunne, J.J., Ong, C.F., DeMers, M.S., Rajagopal, A., Millard, M., Hamner, S.R., Arnold, E.M., Yong, J.R., Lakshmikanth, S.K., Sherman, M.A., Ku, J.P., Delp, S.L., 2018. OpenSim: Simulating musculoskeletal dynamics and neuromuscular control to study human and animal movement. PLoS Comput Biol 14, e1006223.
Shadwick, R., 1990. Elastic energy storage in tendons: mechanical differences related to function and age. Am. J. Physiol. 207, 1033–1040.
Son, J., Ward, S.R., Lieber, R.L., 2024. Scaling relationships between human leg muscle architectural properties and body size. J Exp Biol 227.
Tabary, J.C., Tardieu, C., Tardieu, G., Tabary, C., Gagnard, L., 1976. Functional adaptation of sarcomere number of normal cat muscle. Journal of Physiology (paris) 72, 277–291.
Ward, S.R., Loren, G.J., Lundberg, S., Lieber, R.L., 2006. High stiffness of human digital flexor tendons is suited for precise finger positional control. J Neurophysiol 96, 2815–2818.
Ward, S.R., Eng, C.M., Smallwood, L.H., Lieber, R.L., 2009. Are current measurements of lower extremity muscle architecture accurate? Clin Orthop Relat Res 467, 1074–1082.
Ward, S.R., Winters, T.M., O'Connor, S.M., Lieber, R.L., 2020. Nonlinear scaling of passive mechanical properties in fibers, bundles, fascicles and whole rabbit muscles. Frontiers in Physiology.

Warren, G.L., Ingalls, C.P., Shah, S.J., Armstrong, R.B., 1999. Uncoupling of in vivo torque production from EMG in mouse muscles injured by eccentric contractions. J. Physiol. 515, 609–619.
Wickiewicz, T.L., Roy, R.R., Powell, P.L., Edgerton, V.R., 1983. Muscle architecture of the human lower limb. Clin. Orthop. Relat. Res. 179, 275–283.
Winters, T.M., Takahashi, M., Lieber, R.L., Ward, S.R., 2011. Whole muscle length-tension relationships are accurately modeled as scaled sarcomeres in rabbit hindlimb muscles. J Biomech 44, 109–115.
Zajac, F.E., 1989. Muscle and tendon: properties, models, scaling, and application to biomechanics and motor control. Crit Rev Biomed Eng 17, 359–411.